Cooperative Simultaneous Localization and Synchronization: A Distributed Hybrid Message Passing Algorithm

Bernhard Etzlinger[*], Florian Meyer[†], Andreas Springer[*], Franz Hlawatsch[†], and Henk Wymeersch[‡]

[*]Johannes Kepler University, Linz, Austria, {b.etzlinger, a.springer}@nthfs.jku.at
[†]Vienna University of Technology, Vienna, Austria, {florian.meyer, franz.hlawatsch}@tuwien.ac.at
[‡]Chalmers University of Technology, Gothenburg, Sweden, henkw@chalmers.se

Abstract—**Localization and synchronization in wireless networks are strongly related when they are based on internode time measurements. We leverage this relation by presenting a message passing algorithm for *cooperative simultaneous localization and synchronization* (CoSLAS). The proposed algorithm jointly estimates the locations and clock parameters of the network nodes in a fully decentralized manner while requiring time measurements and communications only between neighboring nodes and making only minimal assumptions about the network topology. Low computation and communication requirements are achieved by a hybrid use of sample-based and Gaussian belief propagation. Our simulations demonstrate performance advantages of the proposed CoSLAS algorithm over separate state-of-the-art localization and synchronization algorithms.**

Index Terms—**Network synchronization, localization, distributed estimation, belief propagation, particle methods, Gaussian message passing, factor graph, CoSLAS.**

I. INTRODUCTION

Locating nodes in large-scale wireless networks is important in many applications [1]. Cooperative self-localization (CSL) algorithms exhibit better coverage and accuracy than traditional noncooperative algorithms [1]–[3]. CSL relies on distance measurements between nodes, which are often extracted from timing measurements. The latter require highly accurate synchronization of nodes [1] or knowledge of clock imperfections [4]. The strong relation between distance and timing estimates suggests that synergies may be leveraged by performing localization and synchronization jointly. Existing approaches to joint CSL and synchronization [5]–[9] place significant constraints on the network topology. Several state-of-the-art algorithms for pure CSL [2], [3] and pure synchronization [10], [11] run a message passing scheme on a factor graph, which avoids these constraints.

In this paper, we present a factor graph formulation of *cooperative simultaneous localization and synchronization* (CoSLAS) that consistently combines the separate factor graphs for CSL and synchronization. We also propose a fully distributed, cooperative belief propagation message passing algorithm that jointly estimates all sensor locations and the frequency and time offsets of all local clocks. This algorithm

is hybrid in that it uses both sample-based and parametric message representations. The algorithm has low requirements regarding the measurement and communication hardware, and the topology constraints are equivalent to those of pure CSL algorithms. In parallel to this work, we also propose a fully sample-based CoSLAS algorithm in [12]. The algorithm in [12] has higher communication requirements while being significantly less complex.

This paper is organized as follows. The system and statistical models are described in Sections II and III, respectively. In Section IV, the CoSLAS factor graph and the corresponding message passing algorithm are presented. Finally, simulation results are discussed in Section V.

II. SYSTEM MODEL

We consider a wireless network of N static nodes, where a node $i \in \mathcal{I} \triangleq \{1, \ldots, N\}$ belongs either to a set $\mathcal{M}$ of synchronous master nodes (MNs) with known locations[1] or to a set $\mathcal{A}$ of asynchronous agent nodes (ANs) with unknown locations, i.e., $\mathcal{I} = \mathcal{M} \cup \mathcal{A}$. The two-dimensional (2D) location of node i is $\mathbf{x}_i = [x_i \ y_i]^{\mathrm{T}}$ and its local clock time is

$$c_i(t) = \alpha_i t + \beta_i . \qquad (1)$$

Here, α_i and β_i are, respectively, the local clock skew and phase offset with respect to the true time t. Both are referred to as the local clock parameters $\boldsymbol{\theta}_i \triangleq [\alpha_i \ \beta_i]^{\mathrm{T}}$.

The abilities for information exchange are represented by the communication set $\mathcal{C} \subseteq \mathcal{I} \times \mathcal{I}$. If two nodes $i, j \in \mathcal{I}$ are able to communicate, then $(i, j) \in \mathcal{C}$ and $(j, i) \in \mathcal{C}$. Without loss of generality, communication between MNs is not considered, i.e., $(i, j) \notin \mathcal{C}$ if $i, j \in \mathcal{M}$. For each $i \in \mathcal{A}$, we define a neighborhood set $\mathcal{T}_i \subseteq \mathcal{I} \setminus \{i\}$ that consists of all $j \in \mathcal{I}$ that communicate with i, i.e. $j \in \mathcal{T}_i$ if and only if $(i, j) \in \mathcal{C}$. We note that unambiguous localization in 2D requires $|\mathcal{T}_i| \geq 3$ $\forall i \in \mathcal{A}$ and $|\mathcal{M}| \geq 3$. An example of a network with $N = 7$ nodes and its connectivity graph are shown in Fig. 1.

Via the communication links, node pairs $(i, j) \in \mathcal{C}$ exchange packets to measure their local clock parameters $\boldsymbol{\theta}_i, \boldsymbol{\theta}_j$ and their distance $d_{ij} \triangleq \|\mathbf{x}_i - \mathbf{x}_j\|$. More specifically, node i transmits $K_{ij} \geq 1$ packets to node j, and node j transmits $K_{ji} \geq 1$
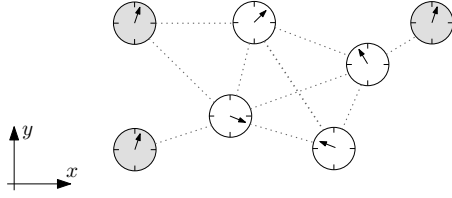
Fig. 1. Connectivity (communication) graph of a wireless network with $|\mathcal{M}| = 3$ MNs (shaded) and $|\mathcal{A}| = 4$ ANs.
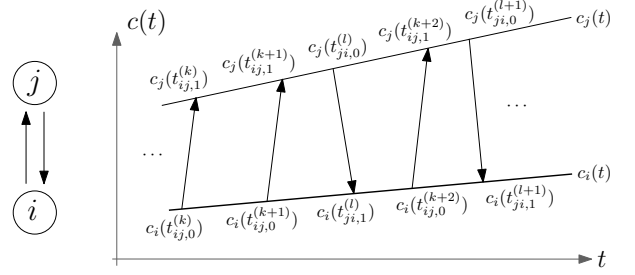

Fig. 2. Local clock functions $c_i(t)$ and $c_j(t)$, local time measurements (time stamps), and corresponding packet transmissions for nodes i and j.

packets to node i. The kth "$i \to j$" packet (where $k \in \{1, \ldots, K_{ij}\}$) leaves node i at time $t_{ij,0}^{(k)}$ and arrives at node j at measured time

$$t_{ij,1}^{(k)} = t_{ij,0}^{(k)} + \delta_{ij}^{(k)}, \quad \text{with } \delta_{ij}^{(k)} = \frac{d_{ij}}{v_0} + u_{ij}^{(k)}. \quad (2)$$

Here, $\delta_{ij}^{(k)}$ is the delay expressed in true time, v_0 is the speed of light, and $u_{ij}^{(k)} \sim \mathcal{N}(0, \sigma_u^2)$ is measurement noise that is modeled as Gaussian and independent across i, j, and k. The transmit and receive times are recorded in local time, resulting in the time stamps $c_i(t_{ij,0}^{(k)})$ and $c_j(t_{ij,1}^{(k)})$. A similar discussion applies to the transmission of the kth packet from node j to node i (where $k \in \{1, \ldots, K_{ji}\}$); the resulting time stamps are $c_j(t_{ji,0}^{(k)})$ and $c_i(t_{ji,1}^{(k)})$. The clock functions $c_i(t)$ and $c_j(t)$ and time stamps are visualized in Fig. 2. A communication protocol ensures that these time stamps are available at both nodes i and j. The aggregated measurement of nodes i and j is thus given by $\mathbf{c}_{ij} \triangleq [\mathbf{c}_{i \to j}^{\mathsf{T}} \ \mathbf{c}_{j \to i}^{\mathsf{T}}]^{\mathsf{T}}$, with $\mathbf{c}_{i \to j} \triangleq \left[c_j(t_{ij,1}^{(1)}) \cdots c_j(t_{ij,1}^{(K_{ij})})\right]^{\mathsf{T}}$ and $\mathbf{c}_{j \to i} \triangleq \left[c_i(t_{ji,1}^{(1)}) \cdots c_i(t_{ji,1}^{(K_{ji})})\right]^{\mathsf{T}}$. For later use, we also define the (recorded, not measured) time stamp vectors $\tilde{\mathbf{c}}_{i \to j} \triangleq \left[c_i(t_{ij,0}^{(1)}) \cdots c_i(t_{ij,0}^{(K_{ij})})\right]^{\mathsf{T}}$ and $\tilde{\mathbf{c}}_{j \to i} \triangleq \left[c_j(t_{ji,0}^{(1)}) \cdots c_j(t_{ji,0}^{(K_{ji})})\right]^{\mathsf{T}}$.

Using (1) and (2), the following relation between the time stamps $c_i(t_{ij,0}^{(k)})$ and $c_j(t_{ij,1}^{(k)})$ is obtained:

$$c_j(t_{ij,1}^{(k)}) = \psi_{i \to j}^{(k)}(\boldsymbol{\theta}_i, \boldsymbol{\theta}_j, d_{ij}) + u_{ij}^{(k)} \alpha_j, \quad (3)$$

with

$$\psi_{i \to j}^{(k)}(\boldsymbol{\theta}_i, \boldsymbol{\theta}_j, d_{ij}) \triangleq \frac{c_i(t_{ij,0}^{(k)}) - \beta_i}{\alpha_i} \alpha_j + \beta_j + \frac{d_{ij}}{v_0} \alpha_j. \quad (4)$$

A similar relation between $c_j(t_{ji,0}^{(k)})$ and $c_i(t_{ji,1}^{(k)})$ is obtained by exchanging i and j in (3), (4).

III. STATISTICAL MODEL

The goal of CoSLAS is to simultaneously estimate the locations $\mathbf{x}_i$ and clock parameters $\boldsymbol{\theta}_i$ of all ANs $i \in \mathcal{A}$ based on the available time stamps between neighboring nodes. Bayesian estimation relies on the posterior distribution of the $\mathbf{x}_i$ and $\boldsymbol{\theta}_i$, which in turn involves the likelihood function and the prior distribution. It will be convenient to consider the distances d_{ij} as further parameters, which are however related to the corresponding node locations as $d_{ij} = \|\mathbf{x}_i - \mathbf{x}_j\|$.

A. Likelihood Function

Because of (3) and the statistical properties of the $u_{ij}^{(k)}$, the local likelihood function of nodes i and j, with $(i, j) \in \mathcal{C}$, is

$$p(\mathbf{c}_{ij} | \boldsymbol{\theta}_i, \boldsymbol{\theta}_j, d_{ij})$$
$$= G_{ij} \exp\left(-\frac{\|\mathbf{c}_{i \to j} - \boldsymbol{\psi}_{i \to j}\|^2}{2\alpha_j^2 \sigma_u^2} - \frac{\|\mathbf{c}_{j \to i} - \boldsymbol{\psi}_{j \to i}\|^2}{2\alpha_i^2 \sigma_u^2}\right),$$

where $G_{ij} \triangleq (2\pi\alpha_j^2\sigma_u^2)^{-K_{ij}/2}(2\pi\alpha_i^2\sigma_u^2)^{-K_{ji}/2}$, $\boldsymbol{\psi}_{i \to j} \triangleq \left[\psi_{i \to j}^{(1)}(\boldsymbol{\theta}_i, \boldsymbol{\theta}_j, d_{ij}) \cdots \psi_{i \to j}^{(K_{ij})}(\boldsymbol{\theta}_i, \boldsymbol{\theta}_j, d_{ij})\right]^{\mathsf{T}}$, and $\boldsymbol{\psi}_{j \to i} \triangleq \left[\psi_{j \to i}^{(1)}(\boldsymbol{\theta}_j, \boldsymbol{\theta}_i, d_{ij}) \cdots \psi_{j \to i}^{(K_{ji})}(\boldsymbol{\theta}_j, \boldsymbol{\theta}_i, d_{ij})\right]^{\mathsf{T}}$. In what follows, it will be convenient to consider the transformed clock parameters $\boldsymbol{\vartheta}_i = [\lambda_i \ \nu_i]^{\mathsf{T}}$ with $\lambda_i \triangleq 1/\alpha_i$ and $\nu_i \triangleq \beta_i/\alpha_i$. As discussed in [11], approximating $\alpha_i^2\sigma_u^2$ and $\alpha_j^2\sigma_u^2$ by σ_u^2 leads to an accurate Gaussian representation in terms of the transformed clock parameters $\boldsymbol{\vartheta}_i$ and $\boldsymbol{\vartheta}_j$:

$$p(\mathbf{c}_{ij} | \boldsymbol{\vartheta}_i, \boldsymbol{\vartheta}_j, d_{ij}) \propto \exp\left(-\frac{\|\mathbf{A}_{ij}\boldsymbol{\vartheta}_i + \mathbf{B}_{ij}\boldsymbol{\vartheta}_j + d_{ij}\mathbf{a}_d\|^2}{2\sigma_u^2}\right),$$
$$(5)$$

with

$$\mathbf{A}_{ij} \triangleq \begin{bmatrix} -\tilde{\mathbf{c}}_{i \to j} & \mathbf{1}_{K_{ij}} \\ \mathbf{c}_{j \to i} & -\mathbf{1}_{K_{ji}} \end{bmatrix}, \quad \mathbf{B}_{ij} \triangleq \begin{bmatrix} \mathbf{c}_{i \to j} & -\mathbf{1}_{K_{ij}} \\ -\tilde{\mathbf{c}}_{j \to i} & \mathbf{1}_{K_{ji}} \end{bmatrix},$$

and $\mathbf{a}_d \triangleq -\frac{1}{v_0}\mathbf{1}_{K_{ij}+K_{ji}}$. Here, $\mathbf{1}_K$ denotes the all-ones vector of dimension K.

Finally, since the measurements $\mathbf{c}_{ij}$ and $\mathbf{c}_{i'j'}$ are conditionally independent unless $(i, j) = (i', j')$, the (approximate) global likelihood function is obtained as

$$p(\mathbf{c} | \boldsymbol{\vartheta}, \mathbf{d}) = \prod_{(i,j) \in \mathcal{C}} p(\mathbf{c}_{ij} | \boldsymbol{\vartheta}_i, \boldsymbol{\vartheta}_j, d_{ij}). \quad (6)$$

Here, $\mathbf{c}$ is the total measurement vector (obtained by stacking all local measurements $\mathbf{c}_{ij}$, $(i, j) \in \mathcal{C}$), $\mathbf{d}$ is the vector of all distances d_{ij}, and $\boldsymbol{\vartheta}$ is the vector of all $\boldsymbol{\vartheta}_i$, $i \in \mathcal{I}$.

B. Prior Distribution

Because the MNs have perfect knowledge of their clock parameters, we use the prior $p(\boldsymbol{\vartheta}_i) = \delta(\boldsymbol{\vartheta}_i - \tilde{\boldsymbol{\vartheta}}_i)$, $i \in \mathcal{M}$, where $\tilde{\boldsymbol{\vartheta}}_i$ denotes the true transformed clock parameter of MN i and $\delta(\cdot)$ denotes the Dirac delta function. For the ANs, we use the Gaussian prior $p(\boldsymbol{\vartheta}_i) = \mathcal{N}(\boldsymbol{\mu}_{\mathrm{p},i}, \boldsymbol{\Sigma}_{\mathrm{p},i})$, $i \in \mathcal{A}$, with $\boldsymbol{\mu}_{\mathrm{p},i} = [1 \ 0]^{\mathsf{T}}$ (note that $\boldsymbol{\vartheta}_i = [1 \ 0]^{\mathsf{T}}$ would correspond to $\alpha_i = 1$ and $\beta_i = 0$) and $\boldsymbol{\Sigma}_{\mathrm{p},i} = \mathrm{diag}\{\sigma_{\lambda_i}^2, \sigma_{\nu_i}^2\}$. As explained in [11], we set $\sigma_{\lambda_i}^2 = \sigma_{\alpha_i}^2$, where $\sigma_{\alpha_i}^2$ is typically given by the oscillator specification, and we choose $\sigma_{\nu_i}^2$ large (resulting in an uninformative prior for $\nu_i = \beta_i/\alpha_i$) since no prior information on the clock phase β_i is available. Because the MNs have also perfect knowledge of their locations, we use

the location prior $p(\mathbf{x}_i) = \delta(\mathbf{x}_i - \tilde{\mathbf{x}}_i)$, $i \in \mathcal{M}$, where $\tilde{\mathbf{x}}_i$ denotes the true location of MN i. For the ANs, $i \in \mathcal{A}$, we have no prior information on the location. Therefore, we use a uniform prior $p(\mathbf{x}_i)$ that covers the whole localization area.

Assuming that all clocks and locations are independent, and recalling that $d_{ij} = \|\mathbf{x}_i - \mathbf{x}_j\|$, we obtain the joint prior of $\mathbf{x} \triangleq [\mathbf{x}_1^{\mathsf{T}} \cdots \mathbf{x}_N^{\mathsf{T}}]^{\mathsf{T}}$, $\boldsymbol{\vartheta}$, and $\mathbf{d}$ as

$$
\begin{aligned}
p(\mathbf{x}, \boldsymbol{\vartheta}, \mathbf{d}) &= p(\mathbf{d}|\mathbf{x})\, p(\mathbf{x})\, p(\boldsymbol{\vartheta}) \\
&= \prod_{(i,j) \in \mathcal{C}} \phi(\mathbf{x}_{ij}, d_{ij}) \prod_{i' \in \mathcal{I}} p(\mathbf{x}_{i'}) p(\boldsymbol{\vartheta}_{i'}), \quad (7)
\end{aligned}
$$

with $\phi(\mathbf{x}_{ij}, d_{ij}) \triangleq \delta(d_{ij} - \|\mathbf{x}_i - \mathbf{x}_j\|)$.

C. Posterior Distribution and Estimators

Using Bayes' rule as well as (6) and (7), we obtain the joint posterior distribution of $\mathbf{x}$, $\boldsymbol{\vartheta}$, and $\mathbf{d}$:

$$
\begin{aligned}
& p(\mathbf{x}, \boldsymbol{\vartheta}, \boldsymbol{d}|\mathbf{c}) \\
& \propto p(\mathbf{c}|\boldsymbol{\vartheta}, \boldsymbol{d})\, p(\mathbf{x}, \boldsymbol{\vartheta}, \boldsymbol{d}) \\
& = \prod_{(i,j) \in \mathcal{C}} \phi(\mathbf{x}_{ij}, d_{ij})\, p(\mathbf{c}_{ij}|\boldsymbol{\vartheta}_i, \boldsymbol{\vartheta}_j, d_{ij}) \prod_{i' \in \mathcal{I}} p(\mathbf{x}_{i'}) p(\boldsymbol{\vartheta}_{i'}). \quad (8)
\end{aligned}
$$

The minimum mean-square error (MMSE) estimates of $\mathbf{x}_i$ and $\boldsymbol{\vartheta}_i$ are given by [13]

$$
\hat{\mathbf{x}}_i = \int \mathbf{x}_i\, p(\mathbf{x}_i|\mathbf{c})\, \mathrm{d}\mathbf{x}_i, \quad \hat{\boldsymbol{\vartheta}}_i = \int \boldsymbol{\vartheta}_i\, p(\boldsymbol{\vartheta}_i|\mathbf{c})\, \mathrm{d}\boldsymbol{\vartheta}_i. \quad (9)
$$

Here, $p(\mathbf{x}_i|\mathbf{c})$ and $p(\boldsymbol{\vartheta}_i|\mathbf{c})$ are obtained from the joint posterior $p(\mathbf{x}, \boldsymbol{\vartheta}, \boldsymbol{d}|\mathbf{c})$ by marginalization, i.e., $p(\mathbf{x}_i|\mathbf{c}) = \int p(\mathbf{x}, \boldsymbol{\vartheta}, \boldsymbol{d}|\mathbf{c})\, \mathrm{d}{\sim}\{\mathbf{x}_i\}$ and $p(\boldsymbol{\vartheta}_i|\mathbf{c}) = \int p(\mathbf{x}, \boldsymbol{\vartheta}, \boldsymbol{d}|\mathbf{c})\, \mathrm{d}{\sim}\{\boldsymbol{\vartheta}_i\}$, where ${\sim}\{y\}$ denotes all variables but y.

IV. DISTRIBUTED PARAMETER ESTIMATION

Since the MMSE estimators in (9) require a marginalization, iterative belief propagation (BP) on a factor graph [14] expressing the factorization structure of the joint posterior in (8) can be used for an efficient approximate computation. In our case, this factor graph can be easily obtained from the connectivity graph (cf. Fig. 1) by the transformation shown in Fig. 3. An example of a basic building block of the resulting CoSLAS factor graph, corresponding to the connection between nodes i and j with $(i,j) \in \mathcal{C}$, is shown in Fig. 4. We note that Fig. 3 and Fig. 4 use the shorthands $\phi_{ij} = \phi(\mathbf{x}_{ij}, d_{ij})$, $p_{ij} = p(\mathbf{c}_{i \to j}|\boldsymbol{\vartheta}_i, \boldsymbol{\vartheta}_j, d_{ij})$, $p_{x,i} = p(\mathbf{x}_i)$, and $p_{\vartheta,i} = p(\boldsymbol{\vartheta}_i)$; furthermore, variable and factor vertices are depicted by circles and rectangles, respectively.

A. Message Passing

At each vertex of the factor graph, messages are calculated according to the BP rules (sum-product algorithm) [14] and passed along the edges of the factor graph to neighboring vertices. In some cases, this requires packet transmissions (these come in addition to the packet transmissions used to measure the time stamps). More specifically, a message from a variable vertex r_i—which may correspond to a vector, e.g., $\mathbf{x}_i$—to a factor vertex f is calculated as
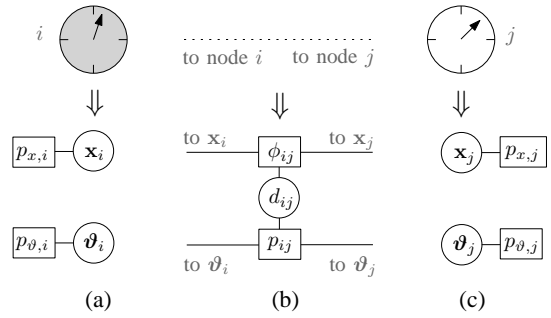

Fig. 3. Transformation of a physical network (connectivity graph) into a factor graph: (a) MN, (b) connection, (c) AN.

$$
m_{r_i \to f}(r_i) \propto \prod_{v \in \mathcal{V}(r_i) \setminus \{f\}} m_{v \to r_i}(r_i), \quad (10)
$$

where $\mathcal{V}(v)$ denotes the set of neighboring vertices of vertex v. Conversely, a message from a factor vertex f to a variable vertex r_i is calculated as

$$
m_{f \to r_i}(r_i) \propto \int f(\mathbf{r}) \prod_{r_j \in \mathcal{V}(f) \setminus \{r_i\}} m_{r_j \to f}(r_j)\, \mathrm{d}{\sim}\{r_j\}, \quad (11)
$$

where the function $f(\mathbf{r})$ corresponds to factor vertex f and $\mathbf{r}$ is the vector of all involved variables (including r_i). An approximation of the marginal posterior of r_i ("belief") is then obtained as

$$
b(r_i) \propto \prod_{f \in \mathcal{V}(r_i)} m_{f \to r_i}(r_i). \quad (12)
$$

Hereafter, we will use the following message naming convention (cf. Fig. 4). Messages that are available at node i and also involve node j will be denoted as $m_{l,ij}^{(q)}$ or $m_{l,ji}^{(q)}$, where l is an identification number, ij indicates messages calculated at node i, ji indicates messages provided by node j to node i via transmission of a packet, and q is the iteration index.

B. Message Representation

We propose a hybrid parametric/nonparametric representation of the various messages. Because the likelihood function in (5) is Gaussian, messages $m_{l,ij}^{(q)}$ linked to the function vertex p_{ij} (see Fig. 4) can be represented by a Gaussian distribution [11], [14], i.e., $m_{l,ij}^{(q)} = \mathcal{N}(\boldsymbol{\mu}_{l,ij}^{(q)}, \boldsymbol{\Sigma}_{l,ij}^{(q)})$ for $l \in \{2, 5, 6, 8\}$. This is a parametric representation in terms of the mean $\boldsymbol{\mu}_{l,ij}^{(q)}$
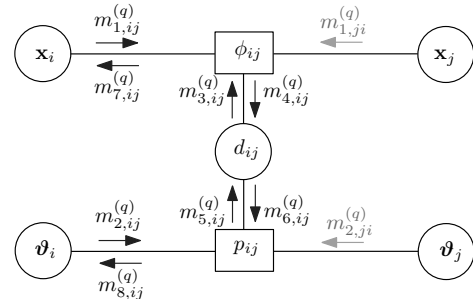

Fig. 4. Example of a building block of the CoSLAS factor graph, corresponding to the connection between nodes i and j with $(i,j) \in \mathcal{C}$.

and the covariance $\boldsymbol{\Sigma}_{l,ij}^{(q)}$ (or variance $\sigma_{l,ij}^{2(q)}$, for $l = 6$). For messages $m_{l,ij}^{(q)}$ linked to the function vertex ϕ_{ij}, because of the nonlinear locations-distance relation expressed by ϕ_{ij}, we use a nonparametric representation [2] by a set of N_s samples (particles) $\mathbf{s}_{l,ij}^{(q,k)}$ and weights $w_{l,ij}^{(q,k)}$, i.e., $m_{l,ij}^{(q)} \stackrel{\triangle}{\approx} \{\mathbf{s}_{l,ij}^{(q,k)}, w_{l,ij}^{(q,k)}\}_{k=1}^{N_s}$ for $l \in \{1, 3, 4, 7\}$. The weights are normalized, i.e., $\sum_{k=1}^{N_s} w_{l,ij}^{(q,k)} = 1$.

Using these representations in (10)–(12) leads to parameter updates as described in [11] and sample updates as described in [2]. The interface between parametric and sample representations is given by the variable vertex d_{ij}. As the incoming message $m_{5,ij}^{(q)}$ is Gaussian, it can be directly sampled, and the parameters of the outgoing message $m_{6,ij}^{(q)}$ are then calculated as the sample mean and sample variance.

C. The CoSLAS Algorithm

Applying the message passing rules with appropriate scheduling leads to the CoSLAS message passing algorithm presented below. The following steps are performed by every AN, whereas MNs only perform the first two steps. Step 1 is the initialization, and steps 2–6 constitute one message passing iteration (with iteration index t). All nodes operate in parallel. Approximations of the estimates (9) can be computed at any iteration q if needed.[2] If a message is not updated during an iteration, it remains unchanged, i.e. $m_{l,ij}^{(q)} = m_{l,ij}^{(q-1)}$.

1) Initialization ($q = 1$): For $i \in \mathcal{I}$ and $j \in \mathcal{T}_i \cap \mathcal{A}$, the messages $m_{1,ij}^{(1)}$ and $m_{2,ij}^{(1)}$ are set equal to the respective location and clock priors. The messages $m_{1,ij}^{(1)}$ are annotated with an "informative" flag, which is true for MNs ($i \in \mathcal{M}$) and false for ANs ($i \in \mathcal{A}$). ANs set $\mu_{6,ij}^{(1)}$ and $\sigma_{6,ij}^{2(1)}$ according to geometrical considerations regarding the distances.

2) Message transmission between nodes: Node $i \in \mathcal{I}$ conveys to its neighbors $j \in \mathcal{T}_i \cap \mathcal{A}$ the messages $m_{2,ij}^{(q)}$ and, if informative, $m_{1,ij}^{(q)}$ via packet transmissions. More specifically, node i transmits to each node $j \in \mathcal{T}_i \cap \mathcal{A}$, $2 + 3$ real values (mean and covariance matrix) corresponding to $m_{2,ij}^{(q)}$ and $2N_s$ real values (N_s equally weighted particles) corresponding to $m_{1,ij}^{(q)}$.

3) Messages from p_{ij} to ϕ_{ij}: For all neighbors $j \in \mathcal{T}_i$ that provide an informative $m_{1,ji}^{(q)}$, AN $i \in \mathcal{A}$ computes $m_{5,ij}^{(q)}$ in Gaussian form (parameters $\boldsymbol{\mu}_{5,ij}^{(q)}$ and $\boldsymbol{\Sigma}_{5,ij}^{(q)}$) and $m_{3,ij}^{(q)}$ in sample form (samples/weights $\{s_{3,ij}^{(q,k)}, w_{3,ij}^{(q,k)}\}_{k=1}^{N_s}$).

4) Messages from ϕ_{ij} to p_{ij}: For all neighbors $j \in \mathcal{T}_i$ for which $m_{1,ij}^{(q)}$ and $m_{1,ji}^{(q)}$ are informative, AN $i \in \mathcal{A}$ computes $m_{4,ij}^{(q)}$ in sample-based form: from equally weighted samples $\mathbf{s}_{1,ij}^{(q,k)}$ and $\mathbf{s}_{1,ji}^{(q,k)}$ representing $m_{1,ij}^{(q)}$ and $m_{1,ji}^{(q)}$, respectively, equally weighted samples representing $m_{4,ij}^{(q)}$ are calculated as $s_{4,ij}^{(q,k)} = \|\mathbf{s}_{1,ij}^{(q,k)} - \mathbf{s}_{1,ji}^{(q,k)}\|$. Subsequently, the mean and variance

representing $m_{6,ij}^{(q)}$ are computed as the sample mean and sample variance, respectively, of $\{s_{4,ij}^{(q,k)}\}_{k=1}^{N_s}$.

5) Marginal belief $b^{(q)}(\mathbf{x}_i)$; messages $m_{7,ij}^{(q)}$ and $m_{1,ij}^{(q+1)}$: At AN $i \in \mathcal{A}$, equally weighted samples $\{\mathbf{s}_{7,ij}^{(q,k)}\}_{k=1}^{N_s}$ representing the incoming message $m_{7,ij}^{(q)}$ from each $j \in \mathcal{T}_i$ providing informative location input are computed as [2]

$$\mathbf{s}_{7,ij}^{(q,k)} = \mathbf{s}_{1,ji}^{(q,k)} + s_{3,ij}^{(q,k)} \begin{bmatrix} \sin(\varphi^{(q,k)}) \\ \cos(\varphi^{(q,k)}) \end{bmatrix}.$$

Here, the $\varphi^{(q,k)}$ are drawn from a uniform distribution on the interval $[0, 2\pi)$. To compute samples $\{\mathbf{x}_i^{(q,k)}\}_{k=1}^{N_s}$ representing the marginal belief $b^{(q)}(\mathbf{x}_i)$ (cf. (12)) and samples $\{\mathbf{s}_{1,ij}^{(q+1,k)}\}_{k=1}^{N_s}$ representing the message $m_{1,ij}^{(q+1)}$ (cf. (10)), several messages represented by sample sets have to be multiplied. This is done by means of [2, Alg. 2], using only informative messages. If the message $m_{1,ij}^{(q+1)}$ can be computed from informative messages of at least one neighbor j' other than j, i.e. $j' \in \mathcal{T}_i \setminus \{j\}$, $m_{1,ij}^{(q+1)}$ is marked as informative.

6) Marginal belief $b^{(q)}(\boldsymbol{\vartheta}_i)$; messages $m_{8,ij}^{(q)}$ and $m_{2,ij}^{(q+1)}$: At AN $i \in \mathcal{A}$, the incoming message $m_{8,ij}^{(q)}$ from each informative neighbor $j \in \mathcal{T}_i$ is computed using standard Gaussian expressions [11]. The marginal belief $b^{(q)}(\boldsymbol{\vartheta}_i)$ and the updated outgoing messages $m_{2,ij}^{(q+1)}$, $j \in \mathcal{T}_i$ are computed according to (12) and (10), respectively. This requires the multiplication of Gaussian messages and a Gaussian prior, which can again be done using standard Gaussian expressions [11].

V. NUMERICAL ANALYSIS

We evaluated the performance of the proposed CoSLAS algorithm on a network consisting of three MNs ($\mathcal{M} = \{1, 2, 3\}$) and four ANs ($\mathcal{A} = \{4, 5, 6, 7\}$). The connectivity graph of the network is as shown in Fig. 1. The node locations are $\mathbf{x}_i = [\xi_i\,\mathrm{m}\ \ \eta_i\,\mathrm{m}]^{\mathrm{T}}$, where ξ_i is the ith element of $\{0, 0, 65, 10, 35, 50, 25\}$ and η_i is the ith element of $\{0, 40, 40, 15, 15, 20, 30\}$. The communication range is $R = 30\,\mathrm{m}$. The number of time stamp transmissions/measurements is $K_{ij} = K_{ji} = 50$, and the measurement noise variance is $\sigma_u^2 = 10^{-15}\,\mathrm{s}^2$. The clock skews α_i were drawn from a Gaussian distribution with mean 1 and standard deviation 10^{-4} ($= 100\,\mathrm{ppm}$), and the phase offsets β_i were drawn from a uniform distribution on the interval $[-1\mathrm{s}, 1\mathrm{s}]$. The messages $m_{6,ij}^{(q)}$ were initialized to $\mu_{6,ij}^{(1)} = 2R/3$ and $\sigma_{6,ij}^{2(1)} = R^2/18$.

In Fig. 5, we compare the performance of the proposed hybrid BP algorithm for CoSLAS (briefly referred to as "CoSLAS-HBP") with the performance of the purely sample-based BP algorithm for CoSLAS proposed in [12] ("CoSLAS-PBP"), of the BP-based synchronization algorithm described in [11] ("Sync-BP"), and of a CSL algorithm that first estimates the clock parameters by running four iterations of the algorithm [11] and then performs hybrid BP-based CSL using these clock parameters[3] ("Sync-Loc-BP"). These results were obtained by averaging over 500 simulation runs (and

---

[2]More specifically, a location estimate can be calculated from the samples $\{\mathbf{x}_i^{(q,k)}\}_{k=1}^{N_s}$ representing the marginal belief $b^{(q)}(\mathbf{x}_i)$ as $\hat{\mathbf{x}}_i^{(q)} = \frac{1}{N_s} \sum_{k=1}^{N_s} \mathbf{x}_i^{(q,k)}$, and estimates of the clock parameters can be obtained from the mean $\boldsymbol{\mu}_i^{(q)}$ of the Gaussian distribution representing the marginal belief $b^{(q)}(\boldsymbol{\vartheta}_i)$ as $\hat{\alpha}_i^{(q)} = 1/\mu_{1,i}^{(q)}$ and $\hat{\beta}_i^{(q)} = \mu_{2,i}^{(q)}/\mu_{1,i}^{(q)}$.

[3]This CSL algorithm corresponds to [2] when distance measurements are obtained via time stamp measurements rather than using perfectly known clocks. Our setting corresponds to a measurement variance of $0.95\,\mathrm{m}^2$ in [2].
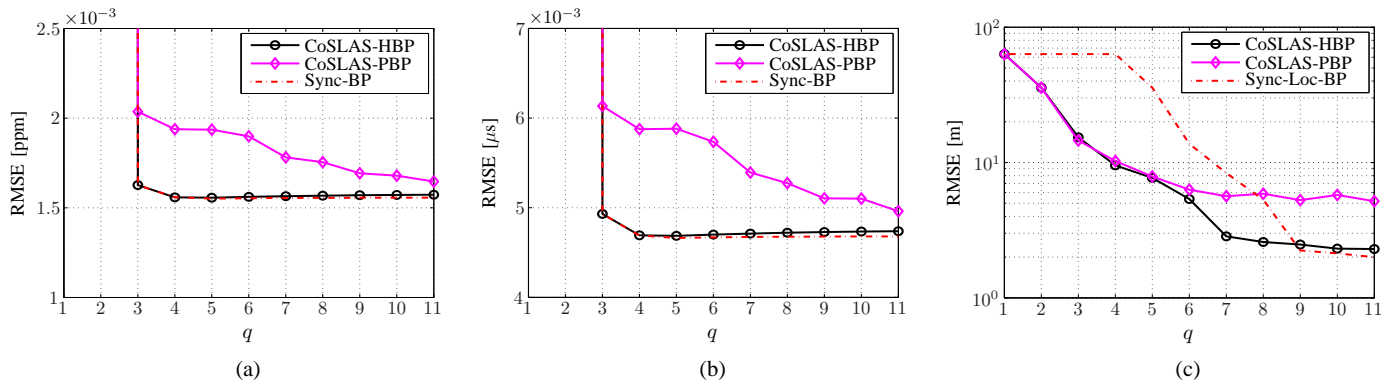
Fig. 5. Average RMSE of (a) clock skew, (b) clock phase, and (c) location versus message passing iteration index q.

measurement noise realizations). The number of samples, N_s, was 1000 for CoSLAS-HBP and 10000 for CoSLAS-PBP. (Note that, despite using ten times more samples, CoSLAS-PBP [12] is significantly less computationally complex than CoSLAS-HBP.) The average root-mean-square-errors (RMSEs) of clock skew estimation, clock phase estimation, and location estimation are shown in Fig. 5(a), (b), and (c), respectively. Looking at the clock RMSEs in Fig. 5(a) and (b), it is seen that the proposed CoSLAS-HBP converges faster than CoSLAS-PBP to the same error floor as Sync-BP. Regarding the location RMSE, one can see from Fig. 5(c) that CoSLAS-HBP eventually achieves a lower RMSE than CoSLAS-PBP. However, further experiments showed that the advantage in localization accuracy of CoSLAS-HBP over CoSLAS-PBP decreases for a growing measurement noise variance (when N_s is fixed). Compared to Sync-Loc-BP, CoSLAS-HBP exhibits a significantly faster convergence to about the same final RMSE.

To summarize, in this setting CoSLAS-HBP outperforms CoSLAS-PBP with respect to both clock and location estimation accuracy. This comes at the cost of a higher computational complexity; however, the communication requirements are lower. In addition, due to the lower dimensionality of the messages and beliefs represented by particles in CoSLAS-HBP compared to CoSLAS-PBP, the required number of particles is smaller by about an order of magnitude; this results in significantly lower memory requirements.

Furthermore, the clock-estimation accuracy of CoSLAS-HBP equals that of Sync-BP and its location-estimation accuracy equals that of Sync-Loc-BP (but with faster convergence). Thus, using the same number of packet transmissions for time measurements as Sync-BP or Sync-Loc-BP, CoSLAS-HBP achieves an equal or better performance while having the advantage of estimating the clocks and locations jointly.

VI. Conclusions

We presented a factor graph framework and a message passing algorithm for distributed cooperative simultaneous localization and synchronization (CoSLAS) in wireless networks. Based on local internode time measurements and communications, the proposed CoSLAS algorithm jointly estimates the locations and clock parameters of the network nodes in a fully decentralized manner while making only minimal assumptions about the network topology. The methodology of factor graphs

and belief propagation is employed to leverage the strong interdependency of localization and synchronization. The use of Gaussian and sample-based message representations results in reduced computation and communication requirements. Numerical simulations show that the proposed CoSLAS algorithm outperforms separate localization and synchronization given the same total number of time measurements.

References

[1] N. Patwari, J. N. Ash, S. Kyperountas, A. O. Hero III, R. L. Moses, and N. S. Correal, "Locating the nodes: Cooperative localization in wireless sensor networks," *IEEE Signal Process. Mag.*, vol. 22, pp. 54–69, Jul. 2005.

[2] A. T. Ihler, J. W. Fisher, R. L. Moses, and A. S. Willsky, "Nonparametric belief propagation for self-localization of sensor networks," *IEEE J. Sel. Areas Commun.*, vol. 23, pp. 809–819, Apr. 2005.

[3] H. Wymeersch, J. Lien, and M. Z. Win, "Cooperative localization in wireless networks," *Proc. IEEE*, vol. 97, pp. 427–450, Feb. 2009.

[4] Y. Wang and W. Xiong, "Improving ranging accuracy of active and passive anchors in the presence of clock imperfection," in *Proc. 10th WPNC*, Dresden, Germany, Mar. 2013.

[5] D. Benoît, J.-B. Pierrot, and C. Abou-Rjeily, "Joint distributed synchronization and positioning in UWB ad hoc networks using TOA," *IEEE Trans. Microw. Theory Techn.*, vol. 54, pp. 1896–1911, Apr. 2006.

[6] J. Zheng and Y.-C. Wu, "Joint time synchronization and localization of an unknown node in wireless sensor networks," *IEEE Trans. Signal Process.*, vol. 58, pp. 1309–1320, Mar. 2010.

[7] S. Zhu and Z. Ding, "Joint synchronization and localization using TOAs: A linearization based WLS solution," *IEEE J. Sel. Areas Commun.*, vol. 28, pp. 1017–1025, Aug. 2010.

[8] S. P. Chepuri, G. Leus, and A.-J. van der Veen, "Joint localization and clock synchronization for wireless sensor networks," in *Proc. Asilomar Conf. Sig., Syst., Comput.*, Pacific Grove, CA, pp. 1432–1436, Nov. 2012.

[9] M. Sun and L. Yang, "On the joint time synchronization and source localization using TOA measurements," *Int. J. Dist. Sensor Netw.*, vol. 2013, Jan. 2013.

[10] M. Leng and Y.-C. Wu, "Distributed clock synchronization for wireless sensor networks using belief propagation," *IEEE Trans. Signal Process.*, vol. 59, pp. 5404–5414, Nov. 2011.

[11] B. Etzlinger, H. Wymeersch, and A. Springer, "Cooperative synchronization in wireless networks." *IEEE Trans. Signal Process.*, 2014, submitted. arXiv:1304.8029v2[cs.DC].

[12] F. Meyer, B. Etzlinger, F. Hlawatsch, and A. Springer, "A distributed particle-based belief propagation algorithm for cooperative simultaneous localization and synchronization," in *Proc. Asilomar Conf. Sig., Syst., Comput.*, Pacific Grove, CA, Nov. 2013.

[13] S. M. Kay, *Fundamentals of Statistical Signal Processing: Estimation Theory*. Upper Saddle River, NJ: Prentice-Hall, 1993.

[14] F. Kschischang, B. Frey, and H.-A. Loeliger, "Factor graphs and the sum-product algorithm," *IEEE Trans. Inf. Theory*, vol. 47, pp. 498–519, Feb. 2001.